The Thesis Committee for Sarah Seraj
Certifies that this is the approved version of the following thesis:

Synthesis of Palladium-Gold Alloy Nanoparticle Catalysts for the Reduction of Nitrite in Water

APPROVED BY
SUPERVISING COMMITTEE:

Supervisor: _____
Charles J. Werth

Co-Supervisor: _____
Simon M. Humphrey

Synthesis of Palladium-Gold Alloy Nanoparticle Catalysts for the Reduction of Nitrite in Water

by

Sarah Seraj, B.S.C.E

Thesis

Presented to the Faculty of the Graduate School of

The University of Texas at Austin

in Partial Fulfillment

of the Requirements

for the Degree of

Master of Science in Engineering

The University of Texas at Austin

May 2016

Dedication

Dedicated to my family: my parents, my sister, my brother-in-law, and my grandparents.

Acknowledgements

I am immensely grateful to my two research advisors, Dr. Charles Werth and Dr. Simon Humphrey, for their feedback, guidance and support. I would also like to thank Pranaw Kunal for mentoring me and for all his contributions to this thesis. I would not have gotten very far without the assistance of my labmates from the Werth Research Group and the Humphrey Research Group. I would particularly like to acknowledge Allison Bergquist, Madison Bertoch, Graham Piburn, Erin Berns, Victoria Boyd, and Julien Botto.

I would like to thank the staff of the Texas Materials Institute and Institute for Cellular and Molecular Biology for their technical assistance. I am also extremely grateful to the National Science Foundation Graduate Fellowship Program and the Cockrell School of Engineering for their financial assistance in graduate school.

I greatly appreciate the support and assistance of the various faculty, staff, and students in the Civil Engineering Department for their support and assistance. I would like to express my gratitude to Dr. Richard Corsi, Dr. Mary Jo Kirisits, and Dr. Paola Passalacqua for their guidance throughout the years, and to Sarah Keithley for teaching me numerous lab techniques.

I would like to thank my family for their unwavering love and support. I want to thank my parents and grandparents for always believing in me, my sister for keeping me on track, and my brother-in-law for his practicality. I would not be where I am now without their encouragement and, sometimes, “tough love”. Finally, I would be remiss not to mention my friends who have helped me get through many stressful times with laughs, advice and love: Shahzad Gani, Manar Hasan, Indu Venu Sabaraya, Nilabh Roy, Eshaba Karim, Osama El-Quqa, Juan Pablo Gevaudan, Sharmistha Maity, Yamit Lavi, Carolyn Joseph, Iktedar Ahmed, Sriramya Nair, and Sydney Mercier.

Abstract

Synthesis of Palladium-Gold Alloy Nanoparticle Catalysts for the Reduction of Nitrite in Drinking Water

Sarah Seraj, M.S.E.

The University of Texas at Austin, 2016

Supervisors: Charles J. Werth and Simon M. Humphrey

Hydrogenation using palladium-based (Pd-based) catalysts has emerged as a promising treatment method for nitrate in drinking water. However, low catalytic activity and longevity can be a barrier to widespread adoption over conventional treatment methods. Controlling catalyst structure at the molecular scale is one approach to improving catalytic activity and longevity. Intermetallic palladium-gold nanoparticle (PdAu NP) alloy catalysts of varying composition were synthesized for nitrite reduction using a polyol reduction method and microwave-assisted heating. The average size of PdAu NPs was 4.1 ± 2.2 nm. Enhanced nitrite reduction has been previously observed for Pd combined with Au in a core-shell NP structure, but has not been studied for intermetallic PdAu alloy NPs. Moreover, the mechanism by which Au enhances Pd-catalyzed nitrite reduction is not well understood. The PdAu NPs were loaded into an amorphous silica support and evaluated for nitrite reduction in a batch reactor. Reaction followed pseudo first-order kinetics for greater than 80% of conversion. Catalyst activity showed volcano-like behavior with varying composition, with the highest activity observed for a Pd:Au molar ratio of 55:45

and a first-order rate constant of 5.77 L min^{-1} g_{metal}^{-1}. All PdAu alloys were significantly more active for nitrite reduction compared to pure Pd NPs, despite Au being catalytically inactive for hydrogenation. Sulfide fouling and catalyst longevity studies were conducted. The presence of Au in the catalyst structure did not appear to enhance resistance to sulfide fouling. Moreover, catalyst activity was reduced upon repeated cycles of nitrite reduction. Further investigation is required to understand the mechanism for catalyst deactivation.

Table of Contents

List of Tables ix

List of Figures x

Chapter 1: Introduction 1

Chapter 2: Experimental Section 6

Materials 6

Catalyst Preparation and Characterization 6

Analytical Methods 8

Kinetic Experiments 9

Kinetic Modeling 10

Chapter 3: Results and Discussion 11

Catalyst Characterization and Performance 11

Sulfide Fouling and Longevity Experiments 15

Chapter 4: Conclusions and Future Work 17

References 19

Vita 23

List of Tables

Table 1: Analytical and catalytic properties of PdAu NPs 11

Table 2: Comparison of results with previous studies on nitrite reduction 13

Table 3: N_2 selectivity at >85% conversion.....14

List of Figures

Figure 1: Proposed nitrate reaction mechanism.....3

Figure 2: Size histograms of PdAuNPs with representative TEM images 12

Figure 3: (A) High-resolution TEM image and (B) elemental mapping of $Pd_{50}Au_{50}$ NP 12

Figure 4: (A) Nitrite reduction profile for $Pd_{50}Au_{50}/SiO_2$ catalyst (B) Metal mass normalized first-order rate constants at different Pd:Au ratios based on elemental analysis in ICP-OES.....13

Figure 5: Nitrate reduction activity of sulfide-fouled $Pd_{50}Au_{50}$ compared to performance under standard conditions.....15

Figure 6: Activity after repeated cycles of nitrite reduction using $Pd_{50}Au_{50}$.....15

Chapter 1: Introduction

Nitrate is one of the most ubiquitous groundwater contaminants in the world (Kapoor and Viraraghavan, 1997). It is regulated by the USEPA at a maximum contaminant level (MCL) of 10 mg/L as N, due to its adverse health effects. Nitrate is known to cause methemoglobinemia (also known as cyanosis or "blue baby syndrome") in infants, a condition where nitrate oxidizes hemoglobin, resulting in inadequate oxygenation in the bloodstream (WHO, 2011a; WHO 2011b). Nitrate has also been attributed to the occurrence of cancer, as it forms carcinogenic N-nitroso compounds in the human body (Weyer *et al*., 2001). Groundwater has low levels of naturally occurring nitrate (NO_3^-), and can have elevated levels due to anthropogenic sources such as nitrogen-containing fertilizers, livestock and septic systems (Dubrovsky and Hamilton, 2010; USEPA, 2007). Since nitrate is both soluble and mobile, it can leach from soils into groundwater (Nolan and Hitt, 2006; ATSDR 2006).

Shallow, rural, domestic wells are the most susceptible to nitrate contamination, particularly those located in agricultural areas (NRC, 1995). Domestic wells are a particular concern because they are not regulated by the Federal Safe Drinking Water Act, and are a source of drinking water for ~46 million Americans (Dubrovsky and Hamilton, 2010). A national analysis of groundwater from 1992 to 2004 by the National Water-Quality Assessment (NAWQA) Program of the United States Geological Survey (USGS) found that nitrate concentrations exceeded the MCL in about 7% of 2,388 sampled domestic wells. A previous NAWQA study reported a nitrate MCL exceedance of 11% in domestic wells (Squillace *et al*., 2002).

The most common method for nitrate removal from drinking water is ion exchange. Ion exchange resins remove nitrate from water, but once the resin capacity is exhausted, they require regeneration with a concentrated brine solution. This results in a secondary waste stream that must be disposed or treated (Clifford and Liu, 1993; Kapoor and Viraraghavan, 1997). Brine accounts for the majority of operational and maintenance costs in ion-exchange systems (Wang *et al*., 2011). A 2.5 MGD (million gallons per day) drinking water plant requires roughly eight tons of salt per day to maintain the system (Choe *et al*., 2015). The regeneration cost over a 20-year plant life can be more than twice that of initial equipment cost (Kapoor and Viraraghavan, 1997). Moreover, the secondary brine waste stream raises additional concerns of maintaining environmental regulations if disposed into sewers or surface waters (Choe *et al*., 2015). Hence, ion exchange results in high environmental impacts and also high costs.

Biological and catalytic treatment of nitrate in drinking water are two emerging technologies for removing nitrate from drinking water. The main drawback to biological denitrification is that long startup times are required to achieve sufficient biomass growth, and this is problematic if treatment is intermittent (Lehman *et al.*, 2008; Ziv-El & Rittmann, 2009). For catalytic treatment, palladium (Pd), rhodium (Rh) and platinum (Pt) are excellent hydrogenation metals and, when used with a promoter metal such as indium (In) or copper (Cu), show good nitrate reduction activity (Marchesini *et al*., 2008; Soares, Órfão, & Pereira, 2008; Witońska, Karski, & Gołuchowska, 2007; Pintar *et al*., 1996).

The proposed reaction mechanism for catalytic nitrate reduction is shown below (Chaplin *et al*., 2012). Both a hydrogenation metal and a promoter metal are required for the first step of nitrate reduction to nitrite. All the remaining steps require only the hydrogenation metal. The two end products of catalytic nitrate reduction are dinitrogen (N_2) and ammonia (NH_3). Pd, combined with either copper (Cu) or indium (In), has been shown to provide the most active catalysts for nitrate reduction, and the most selective for N_2 (Chaplin *et al*., 2012). Pt or Rh, in place of Pd, shows similar activity, but more selectivity for NH_3. Among the promoter metals, In has emerged as the preferred promoter metal, because it is more stable than Cu (Chaplin *et al*., 2007). Pd and In are typically loaded onto a catalyst support to facilitate handling and incorporation into packed-bed reactors, and in some cases, this increases catalytic activity. Carbon-based supports such as activated carbon or graphite, and ceramic-based supports such as alumina or silica, are common. Carbon-based supports are reported to have higher selectivity for NH_3 during nitrite reduction (Chinthaginjala & Lefferts, 2010). Typically, N_2 is the desired end product, because it is innocuous compared to NH_3. However, recovery of NH_3 could add economic value to the cost of treatment if converted to fertilizer.

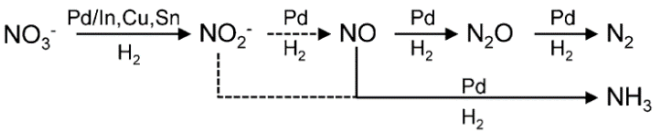

Figure 1: Proposed nitrate reaction mechanism (Chaplin et al., 2012)

Among the primary challenges to developing an economically and environmentally sustainable catalytic treatment technology for nitrate, either for direct water treatment or nitrate contaminated brine, are enhancing catalyst activity and longevity (Choe *et al*., 2015; Bergquist *et al*., 2016). Efforts to address these challenges have focused on tailoring catalyst design at the molecular scale, and include controlling the dispersion of Pd and the

promoter metal (eg. In, Cu, Sn) on a variety of supports (Marchesini *et al*., 2008; Garron, Lázár, & Epron, 2006), using novel supports with unique electronic properties (Chinthaginjala *et al*., 2010; Shuai *et al*., 2012), creating shape- and size- controlled Pd nanoparticles (NPs) (Shuai *et al*., 2013), and combining Pd with catalytically inactive metals (e.g., Au) to enhance hydrogenation activity (Qian *et al*., 2014). Recent efforts in the last category have primarily focused on synthesizing highly active core-shell nanoparticles (Zhao *et al*., 2013), where a Pd shell is loaded onto an Au NP core to enhance reduction of the intermediate nitrite to dinitrogen. Wong and co-workers first demonstrated enhanced reactivity of Pd-on-Au NPs (compared to pure Pd) for aqueous-phase dechlorination reactions (Pretzer *et al*., 2013; Zhao *et al*., 2013), and more recently for nitrite reduction (Qian *et al*., 2014). Moreover, the presence of Au in PdAu alloys may increase resistance to sulfide poisoning by inhibiting formation of the sulfide phase, Pd_4S (Venezia *et al.*, 2003).

An emerging alternative to core-shell NPs is to create intermetallic alloys to enhance Pd hydrogenation activity. While such materials have been examined for gas phase reactions (e.g., Chen *et al.,* 2005), they have not been extended to evaluation of aqueous phase reactions, including nitrate and nitrite reduction. Alloyed or intermetallic structures take advantage of d-band intermixing and ensemble effects between two or more metals in order to improve reactivity at the NP surface; the relative amounts of each metal can be adjusted for a specific catalytic purpose (Garcia *et al*., 2014; Liu *et al*., 2001; Sinfelt, 1977). For example, Garcia *et al*. (2014) alloyed rhodium (Rh) with silver (Ag) and Au to produce catalysts that had up to fifteen times higher activity for cyclohexene hydrogenation

compared to pure Rh, despite Au and Ag being catalytically inactive for hydrogenation. Theoretical modelling showed that this was because the overall reaction energy profile was optimized due to d-band intermixing of Rh with Ag and Au.

The goals of this work are to develop the first highly active PdAu alloy catalyst for nitrite reduction, and to determine the mechanisms of this enhancement. A novel microwave-assisted synthesis method that allows for much greater control over NP structure compared to conventional heating methods was used (Dahal *et al*., 2012). NPs with Pd:Au ratios from 5:1 to 1:2 were synthesized, and characterized using low and high resolution transmission electron microscopy (TEM) and energy-dispersive X-ray spectroscopy (EDS). Turn over frequencies (TOF) for nitrite reduction in aqueous media were determined from batch experiments and compared to literature results to identify mechanisms of rate enhancement. Catalyst longevity was evaluated by subjecting the most active alloy catalyst to sulfide, a known foulant, and to repeated cycles of treatment. Deactivation mechanisms were probed with the aforementioned characterization tools.

Chapter 2: Experimental Section

Materials

Potassium tetrachloropalladate (K_2PdCl_4, 99%; Strem Chemicals), chloroauric acid ($HAuCl_4$, 99.9%; Strem Chemicals), poly(vinylpyrrolidone) ($\{C_6H_9NO\}_n$, $<M_w> = 58\ 000$; Alfa Aesar), ethylene glycol ($\{CH_2OH\}_2$, 99.8%; Fisher Scientific) and sodium borohydride ($NaBH_4$, 98%; Alfa Aesar) were used for the microwave-assisted NP synthesis reaction. Pluronic P123 (poly (ethylene glycol), $<M_w> = 5\ 800$; Sigma Aldrich), hydrochloric acid (12.1 M; Fisher Scientific), n-decane ($CH_3(CH_2)_8CH_3$, 99%; Acros Organics), ammonium fluoride (NH_4F, 96%, Alfa Aesar), and tetraethyl orthosilicate ($Si(OC_2H_5)_4$, 98%: Alfa Aesar) were used to prepare the amorphous silica support. Sodium nitrite ($NaNO_2$, 99%; Sigma Aldrich) was used as the nitrite source in the kinetic experiments, while sodium sulfide nonahydrate ($Na_2S{\cdot}9H_2O$, 98%; Sigma Aldrich) was used as the sulfide source in the sulfide fouling experiments. Potassium dihydrogen phosphate (KH_2PO_4, 99%; Sigma Aldrich) and potassium hydrogen phosphate (K_2HPO_4, 98%; Sigma Aldrich) were used to control pH in the kinetic experiments. H_2 gas (99.9%; Praxair) was used as the elector donor in kinetic experiments. All solvents and reagents were analytical grade, unless stated otherwise.

Catalyst Preparation and Characterization

The catalysts used in this work were Pd_xAu_{100-x} alloy NPs supported on an amorphous silica support. The variable 'x' represents the molar percent of Pd in the alloy, and varied from 0 to 100. The NPs were synthesized via a polyol reduction method with microwave-assisted heating, using previously published methods (Garcia *et al*.,2014; Garcia *et al*., 2013; Dahal *et al.,2012*). Advantages of using microwave-assisted heating

include the production of nanosized “hotspots” in solution that are considered to be much hotter than the temperature of the bulk solvent (Dahal *et al*., 2012). These hotspots are favorable zones for NP nucleation, producing highly homogenous and crystalline nucleates (Garcia *et al*., 2014).

For NP synthesis, a solution of excess PVP (*poly*(vinylpyrrolidone); 225 mg) in ethylene glycol (15 ml) was first heated to 150°C via microwave-assisted heating (MwH) under vigorous magnetic-stirring. A MARS 5 (CEM Corp.) microwave system with a maximum power of 1600 W (2.45 GHz) was used, and the temperature was controlled via a fiber-optic temperature sensor (RTP300+). Ethylene glycol served as both the reaction medium and reductant, and PVP served as a stabilizer. Sodium borohydride (5.6 equivalents per Au) was employed as a secondary reductant for Au(III) and was added along with the ethylene glycol and PVP. The metal precursors (K_2PdCl_4 and $HAuCl_4$ for Pd and Au respectively) were prepared in a separate solution of 2.5 ml ethylene glycol, and added to the hot solvent with a syringe pump at 300 ml/min. The amount of metal precursors was selected based on the desired stoichiometric ratio of Pd:Au in each reaction, with the total metal content kept constant at 0.1 mmol. After a 5 min reaction under continuous MwH at 150°C, the reaction flask (50 ml round bottom flask, attached to a water-based reflux condenser) was submerged in an ice-water bath to quench the reaction. After cooling, the NPs were precipitated by the addition of acetone (72.5ml) and isolated by centrifugation (5500 rpm, 5 min). The supernatant was poured off, and the remaining solid was washed with ethanol (15 ml) using sonication (1 min). Hexane was added (75 ml) to the ethanol-NP suspension, followed by another round of centrifugation. After pouring off the supernatant, the NPs were allowed to air-dry overnight.

Amorphous silica (SiO_2) support was prepared similarly to a previously reported method (Dahal, Ibarra & Humphrey, 2012). Briefly, Pluronic P123 (2.40 g) was stirred into

HCl (85 ml; 1.03 M) solution, followed by *n*-decane (25 ml; 87.2 mmol), which served as a swelling agent. After stirring for 1-2 hours, ammonium fluoride catalyst (0.028 g; 0.76 mmol) and tetraethyl orthosilicate (5.6 ml; 25.2 mmol) were added. The stirring was continued for another 24 hours at 40°C. The resulting opaque slurry was decanted into a bottle, heated at 100°C for 48 hours, and then filtered. Excess surfactant was removed by washing with ethanol, followed by calcination at 550°C for 5 hours. The Pd:Au NPs were loaded into the silica support through impregnation in 1:1 ethanol-water suspensions, followed by oven-drying at 70°C for 12 hours. When loading the NPs into the support, the mass ratio of support to NP was 7.5:1, to obtain metal mass loadings of 0.7-1.8%.

Analytical Methods

Nitrite concentrations were analyzed by ion chromatography (Dionex ICS-2100; Dionex IonPac AS19 column; 32mM KOH eluent; 1 mL/min eluent flow rate). Ammonia concentrations were measured with Hach colorimetric kits (Salicylate method; 0.02 to 2.50 mg/L NH_3-N). Metal loading and elemental analyses of the supported catalysts were determined by ICP-OES (Agilent; Varian 710). Samples were prepared for ICP-OES by digesting 5 mg of catalyst in 10 ml aqua regia. After 12 hours of dissolution, the aqua regia was boiled off to <5ml to ensure complete digestion of metals. The solution was filtered to remove the silica support and diluted with 2% HCl acid before analysis. The measurement of pH and temperature was performed with a temperature-adjusted pH electrode (Radiometer Analytical; PHC3081-8).

Average NP size was measured from low-resolution Transmission Electron Microscopy (TEM) images (FEI Technai, 80kV) of at least 300 particles. TEM grids (Formvar/carbon 200 mesh, copper; Ted Pella) were prepared by drop-casting ethanol

suspensions of catalyst onto the grid, which was then air-dried. High-resolution TEM (HRTEM) images were obtained using a JEOL 2010F transmission electron micro- scope, operated at 200 keV.

Kinetic Experiments

Nitrite reduction experiments lasted 2.5 hours and were conducted at constant temperature (22±1°C) and atmospheric pressure under magnetic stirring in a septum-sealed glass batch reactor (60 ml). The reaction medium contained phosphate buffer (40 ml) amended with the prepared catalyst (0.5 g/L). The phosphate buffer maintained a pH of 6.4. The suspension was pre-sparged with hydrogen for one hour to saturate the water and headspace, and then the reaction was initiated with a 100µl aliquot addition of 0.87M nitrite for an initial concentration of 100 mg/L as NO_2^-. Samples were taken at regular time intervals for analysis; the total sample volume removed was ≤10% of total solution volume. Since the catalyst suspension was homogenous in the reactor, it was assumed that the catalyst concentration in the reactor remained approximately constant.

The kinetic experiments for sulfide fouling were performed in a similar method. However, $Na_2S(9H_2O)$ was added and allowed to mix with the catalyst for 1 hr before sparging the catalyst-amended reaction medium with H_2, and then amending with the aliquot of concentrated nitrite solution to initiate reaction. A loading of 1.2 mmol S/g Pd was targeted, because this amount of sulfide resulted in intermediate but not complete catalyst fouling of a monometallic Pd catalyst in prior work (Chaplin *et al*., 2007).

Catalyst longevity was evaluated by conducting five sequential nitrite reduction experiments with the same catalyst. At the end of each reduction reaction experiment, the catalyst-amended solution was re-sparged with H_2 for an hour, and then amended with a

new aliquot of nitrite (100 mg/L) solution. As before, it was assumed that the catalyst concentration in the reactor remained approximately constant because samples were removed from a well-mixed reactor (i.e., catalyst mixed well with solution). Triplicate experiments were performed for each unique catalyst composition. Sulfide fouling and longevity experiments were conducted on the $Pd_{50}Au_{50}/SiO_2$ catalyst, and were performed in duplicate.

Kinetic Modeling

Nitrite reduction followed pseudo first-order kinetics for greater than 80% of initial nitrite concentration removal. Observed first-order rate constants normalized by metal concentration for each catalyst were obtained from linear regressions of the natural log of concentration versus time plots from the following equation:

$$-\frac{dC_{NO_2^-}}{dt}\left(\frac{1}{C_{met}}\right) = k_{obs} C_{NO_2^-} \qquad \text{(Eq. 1)}$$

Where $C_{NO_2^-}$ represents the aqueous nitrite concentration (mg NO_2^-/L), C_{met} represents the concentration of metal in the catalyst (g_{met}/L), and k_{obs} is the observed first-order rate constant normalized by metal concentration (L g_{met}^{-1} min^{-1}). The first-order kinetic model was used in lieu of more complicated rate expressions to facilitate comparison with literature values.

Chapter 3: Results and Discussion

Catalyst Characterization and Performance

The theoretical and measured ratios of Pd:Au for each of the synthesized catalysts are shown in Table 1. The results show that the Pd:Au molar ratios from ICP-OES agreed well with the theoretical values. The alloys were consistently more Pd-rich than the intended Pd atomic %; the maximum percent difference between target Pd atomic % and measured values is 12%. The metal mass loading obtained on the silica supports ranged from 0.7-1.8% by weight.

The average size of PdAu NPs was 4.1 ± 2.2 nm, and the sizes obtained at each composition are listed in Table 1. TEM images of the NPs show well-defined structures, which are near mono-disperse (Figure 2). Particles became smaller, and more uniform as the Au content increases up to 45 at%, with a smaller spread of particle sizes. Above 45 at%, NP sizes increases with Au content. Pd-rich particles had a greater tendency to aggregate, indicating that Au plays a role in the stabilization of the NPs.

Table 2: Analytical and catalytic properties of PdAu NPs

	ICP-OES wt %*		ICP-OES Molar %*		Size**	Rate constant†
	Pd	Au	Pd	Au	(nm)	(L/min*g metal)
Pd	1.38	0	100	0	9.5 ± 3.4	2.25 ± 0.35
$Pd_{84}Au_{16}$	1.15	0.37	85	15	7.0 ± 2.5	3.83 ± 0.52
$Pd_{75}Au_{25}$	0.72	0.42	76	24	4.0 ± 1.4	4.05 ± 0.48
$Pd_{67}Au_{33}$	0.74	0.53	72	28	4.0 ± 1.4	4.05 ± 0.46
$Pd_{50}Au_{50}$	0.28	0.43	55	45	2.1 ± 0.6	5.77 ± 0.52
$Pd_{33}Au_{67}$	0.30	0.95	37	63	3.3 ± 1.0	3.16 ± 0.33
Au	1.83	0	0	100	18.2 ± 7.4	0.01 ± 0.01

*ICP results are from NP supported on amorphous silica.

**Size was measured by taking the average of 300 particles from TEM images.

†Rate constants from nitrite reduction reactions are normalized to the total amount of metal in each catalyst and are provided with their 95% confidence intervals.

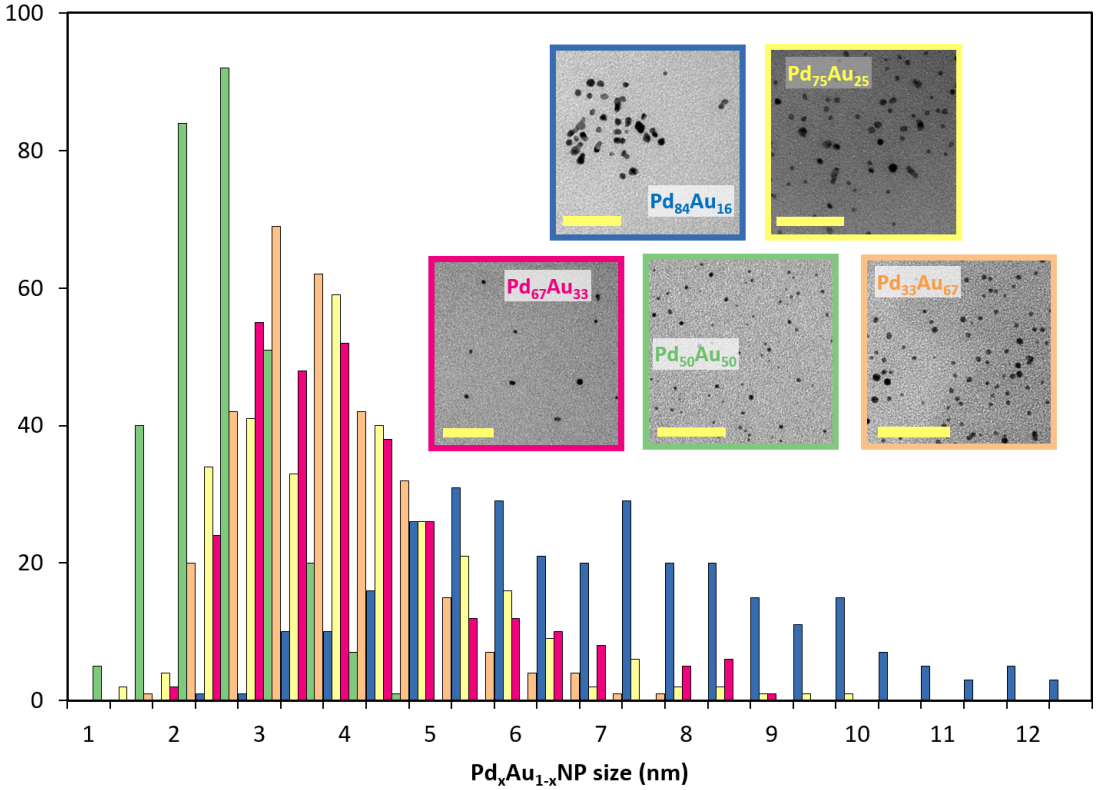

Figure 2: Size histograms of PdAu NPs with representative TEM images (inset; scale bars = 50nm)

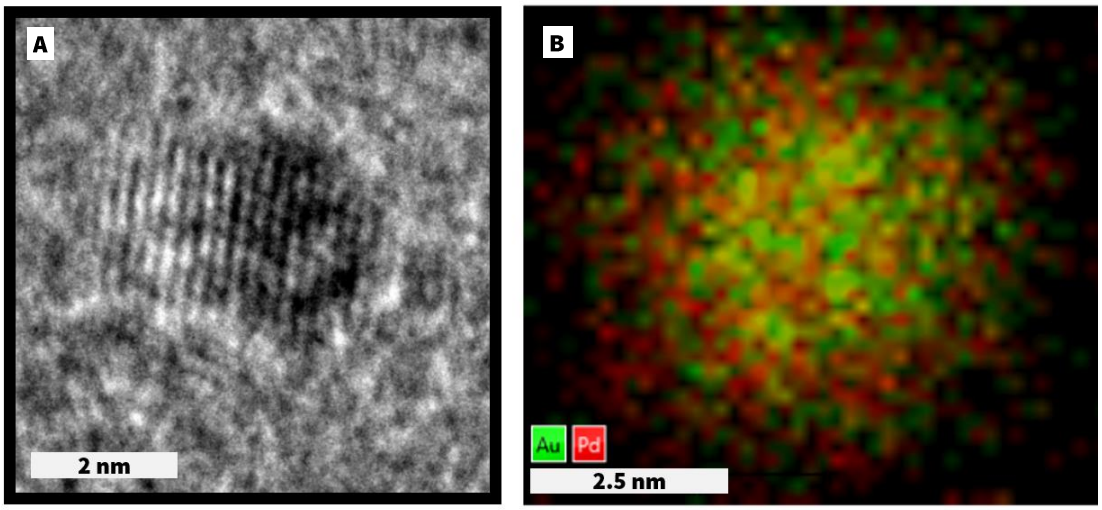

Figure 3: (A) High-resolution TEM image and (B) elemental mapping of $Pd_{50}Au_{50}$ NP

A high resolution TEM image of an individual unsupported $Pd_{50}Au_{50}$ NP is provided in Figure 3A. The corresponding elemental mapping of an unsupported $Pd_{50}Au_{50}$ NP indicates uniform alloying between Pd and Au, with no discernable segregation of Pd and Au (Figure 3B).

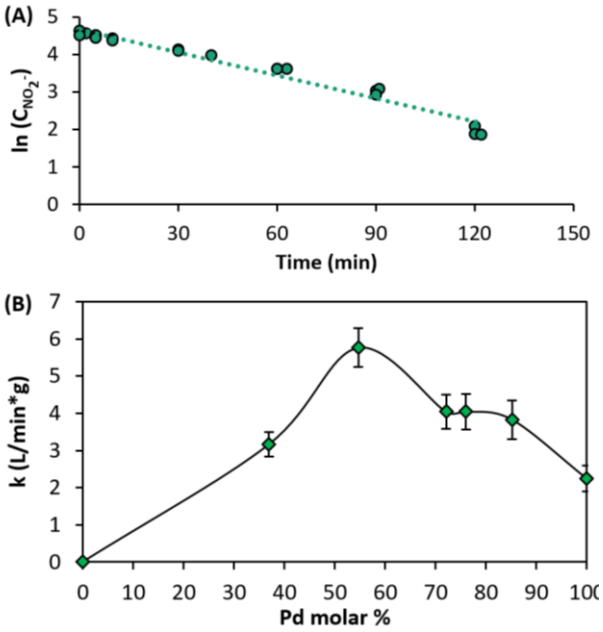

Figure 4: (A) Nitrite reduction profile for $Pd_{50}Au_{50}/SiO_2$ catalyst (B) Metal mass normalized first-order rate constants at different Pd:Au ratios based on elemental analysis in ICP-OES

A representative nitrite reduction profile of the $Pd_{50}Au_{50}/SiO_2$ catalyst is shown in Figure 4A. Pseudo first-order kinetics is observed for the first 80% of reduction. Apparent first-order rate constants were determined from nitrite reduction profiles, and they are plotted versus Pd:Au ratios in Figure 4B. The

Table 2: Comparison of results with previous studies on nitrite reduction

Catalyst	Metal wt%	k_{obs} ($L\ g_{met}^{-1}\ min^{-1}$)	Catalyst conditions	Synthesis	Source
$Pd_{50}Au_{50}/SiO_2$	Pd 0.28%, Au 0.43%	5.77	Supported alloy NP catalyst	Ethylene glycol reduction	This study
80 sc% Pd-on-Au NPs	Pd 15.5%, Au 84.5%	89	Core-shell NP; colloidal dispersion	Citrate/tannic acid reduction	Qian *et al* ., 2014
$Pd_{80}Cu_{20}/PVP$	Pd 85.5%, Au 14.4%	1.67	Alloy NP; colloidal dispersion	2-Ethoxyethanol reduction	Guy *et al* ., 2009
$Pd/\gamma\text{-}Al_2O_3$	Pd 5%	4.43	Bulk supported catalyst	Purchased; Sigma-Aldrich	Shuai *et al* ., 2010
$Pd\text{-}In/\gamma\text{-}Al_2O_3$	Pd 5%, In 0.5%	6.93	Bulk supported catalyst	Incipient wetness	Shuai *et al* ., 2010

catalyst activity shows volcano-like behavior, with the highest activity observed for the

$Pd_{50}Au_{50}/SiO_2$ with a Pd:Au molar ratio of 55:45, and no activity observed for the Au only catalyst. The corresponding rate constant for the $Pd_{50}Au_{50}/SiO_2$ catalyst is 5.77 L min^{-1} g_{met}^{-1}. All PdAu alloys were significantly more active for nitrite reduction compared to pure Pd NPs, despite Au being catalytically inactive for hydrogenation. It is interesting to note the correlation of particle size and mono-dispersity with catalyst activity; highest activity was obtained for the catalyst with smallest NP size ($Pd_{50}Au_{50}/SiO_2$).

The metal normalized first-order rate constant for the $Pd_{50}Au_{50}$-SiO_2 catalyst is compared to literature values in Table 2. Most values are similar to this study, even though a variety of catalyst types are represented. These include an unsupported Pd-Cu alloy catalyst (Guy *et al*., 2009), a commercial Pd/γ-Al_2O_3 catalyst (Shuai *et al*., 2010), and a Pd-In/γ-Al_2O_3 catalyst prepared by incipient wetness. The exception is the rate constant determined using an unsupported NP catalyst comprised of an Au core decorated by a Pd shell (Qian *et al*., 2014). This rate constant is an order of magnitude higher than all other studies, including ours.

Nitrite reduction selectivity for N_2 was measured and results are shown in Table 3. For all Pd:Au alloy combinations, and for the pure Pd, N_2 selectivity was greater than 98%. This was similar to previously reported values for nitrite reduction using Pd-based catalysts (Qian *et al*., 2014; Guy *et al*., 2009).

Table 3: N_2 selectivity at >85% conversion

Catalyst	% N_2
Pd	99.3
$Pd_{84}Au_{16}$	99.1
$Pd_{75}Au_{25}$	>99.9
$Pd_{67}Au_{33}$	99.2
$Pd_{50}Au_{50}$	99.4
$Pd_{33}Au_{67}$	98.7

Sulfide Fouling and Longevity Experiments

Nitrite reduction in the presence and absence of sulfide was measured on the $Pd_{50}Au_{50}/SiO_2$ and Pd/SiO_2 catalyst, and results are shown in Figure 5. Apparent first-order rate constants are shown in the inset. The activity of the sulfide-fouled $Pd_{50}Au_{50}/SiO_2$ catalyst was reduced to 44% of that on the fresh catalyst. The deactivation of the sulfide-fouled Pd/SiO_2 catalyst was similar, and its activity was reduced to 54% of that on the fresh catalyst. We did not observe increased resistance to sulfide poisoning due to the presence of Au, in contrast to Venezia *et al*. (2003).

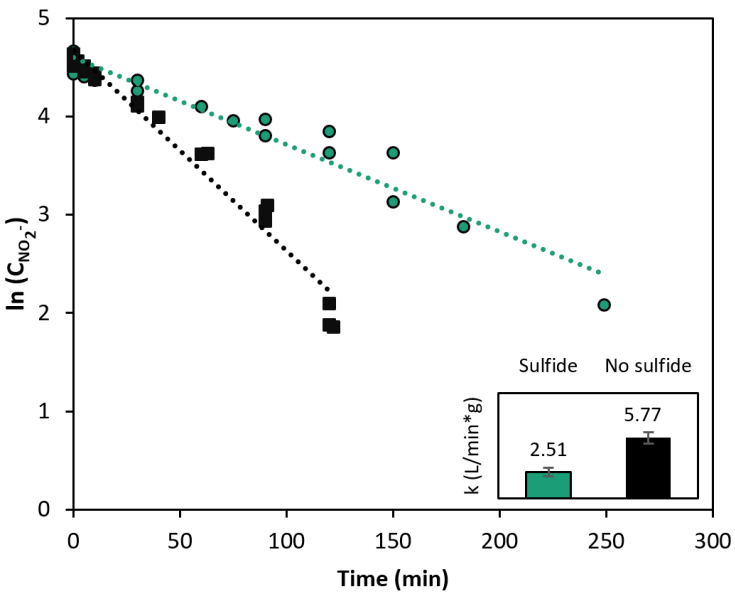

Figure 5: Nitrate reduction activity of sulfide-fouled $Pd_{50}Au_{50}/SiO_2$ compared to performance under standard conditions

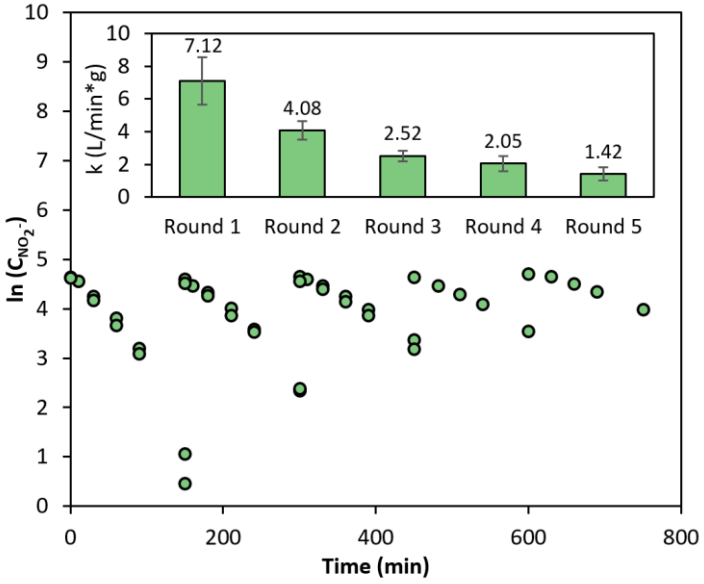

Figure 6: Activity after repeated cycles of nitrite reduction using $Pd_{50}Au_{50}/SiO_2$

Further investigation is needed to determine if sulfide is only bound to Pd, or if sulfide bound to Au is decreasing catalyst activity.

Nitrite reduction was measured using the $Pd_{50}Au_{50}/SiO_2$ catalyst over five sequential cycles, where fresh nitrite was amended to solution at the start of each cycle to obtain the same initial nitrite concentration (Figure 6). Apparent first-order rate constants determined for each cycle are shown in the inset. A reduction in activity is apparent from the nitrite reduction profiles, and from the first-order rate constants. By the third cycle, the catalyst had only 35% of its original activity, and by the fifth cycle this had reduced to 20%. The reason for deactivation is not clear, and is currently under investigation. It is hypothesized that alloy segregation occurred, with the surface becoming more Au-rich, leading to a reduction in the number of active Pd sites.

Chapter 4: Conclusions and Future Work

Silica-supported PdAu alloy NPs were significantly more active for nitrite reduction compared to pure silica-supported Pd NPs, despite Au being catalytically inactive for hydrogenation. The best catalyst activity was achieved at a Pd:Au molar ratio of 55:45, which is close to the optimum ratios obtained for PdAu-catalyzed cyclohexene hydrogenation in previous work (Kunal *et al*., 2016, submitted). Surprisingly, catalyst activity decreased in the presence of sulfide and over repeated cycles of treatment. It is possible that restructuring of the PdAu alloy occurred under reaction conditions, with migration of Au to the surface, reducing the number of active Pd sites. The possible restructuring or segregation of the PdAu alloy under reaction conditions is currently under investigation.

While this project focused on gaining better mechanistic insights into the enhancement of Pd-catalyzed nitrite hydrogenation reactions when it is alloyed with Au, the ultimate objective is to create highly active catalysts for nitrate reduction, which requires a promoter metal. The promoter metal can be substituted into the metal alloy or added to the support as separate discrete NPs. There is also the possibility of using a promoter metal as a support (eg. indium (III) oxide) and decorating it with Pd or PdAu NPs. Exploring different ways to incorporate the promoter metal will be another aspect of our future work.

Finally, we will be using DFT to model optimum alloy compositions for nitrate/nitrite hydrogenation and compare with experimental results from our study. DFT can be used to calculate the d-band center of different metal alloy compositions, and, in theory, the composition of metals can be tuned to optimize the binding energy at the metal-

metal interface for different adsorbates in order to develop novel catalyst materials (Garcia *et al*., 2014).

References

Agency for Toxic Substances and Disease Registry (2006). Interaction profile for atrazine, diethylatrazine, diazinon, nitrate, and simazine. Atlanta GA: US Department of Health and Human Services, Public Health Service.

Agency for Toxic Substances and Disease Registry (2011). Case Studies in Environmental Medicine, Nitrate/Nitrite Toxicity, U.S. Department of Health and Human Services.

Bergquist, A. M., Choe, J. K., Strathmann, T. J., & Werth, C. J. (2016). Evaluation of a hybrid ion exchange-catalyst treatment technology for nitrate removal from drinking water. *Water Research, 96*, 177–187.

Chaplin, B. P., Reinhard, M., Schneider, W. F., Schüth, C., Shapley, J. R., Strathmann, T. J., & Werth, C. J. (2012). Critical review of Pd-based catalytic treatment of priority contaminants in water. *Environmental Science and Technology*, *46*(7), 3655–3670.

Chaplin, B. P., Shapley, J. R., & Werth, C. J. (2007). Regeneration of sulfur-fouled bimetallic Pd-based catalysts. *Environmental Science and Technology*., *41*(15), 5491–5497.

Chaplin, B. P., Roundy, E., Guy, K. A., Shapley, J. R., & Werth, C. J. (2006). Effects of Natural Water Ions and Humic Acid on Catalytic Nitrate Reduction Kinetics Using an Alumina Supported Pd - Cu Catalyst. *Environmental Science & Technology*, *40*(9), 3075–3081.

Chen, M., Kumar, D., Yi, C.-W., & Goodman, D. W. (2005). The promotional effect of gold in catalysis by palladium-gold. *Science (New York, N.Y.)*, *310*(5746), 291–293.

Chinthaginjala, J. K., & Lefferts, L. (2010). Support effect on selectivity of nitrite reduction in water. *Applied Catalysis B: Environmental*, *101*(1-2), 144–149.

Choe, J. K., Bergquist, A. M., Jeong, S., Guest, J. S., Werth, C. J., & Strathmann, T. J. (2015). Performance and life cycle environmental benefits of recycling spent ion exchange brines by catalytic treatment of nitrate. *Water Research, 80*, 267–280.

Clifford, D., & Liu, X. (1993). Ion Exchange for Nitrate Removal. *American Water Works Association, 85*(4), 135–143.

Cuenya, B. R. (2010). Synthesis and catalytic properties of metal nanoparticles: Size, shape, support, composition, and oxidation state effects. *Thin Solid Films*, *518*(12), 3127–3150.

Dahal, N., García, S., Zhou, J., & Humphrey, S. M. (2012). Beneficial effects of microwave-assisted heating versus conventional heating in noble metal nanoparticle synthesis. *ACS Nano*, *6*(11), 9433–9446.

Dahal, N., Ibarra, I. A., & Humphrey, S. M. (2012). High surface area mesoporous Co3O4 from a direct soft template route. *Journal of Materials Chemistry*, *22*, 12675–12681.

Dubrovsky, N., Hamilton, P. (2010). Nutrients in the nation's streams and groundwater: national findings and implications. Reston (VA): United States Department of the Interior, United States Geological Survey.

García, S., Anderson, R. M., Celio, H., Dahal, N., Dolocan, A., Zhou, J., & Humphrey, S. M. (2013). Microwave synthesis of Au-Rh core-shell nanoparticles and implications of the shell thickness in hydrogenation catalysis. *Chemical Communications*, *49*(39), 4241–3.

García, S., Zhang, L., Piburn, G. W., Henkelman, G., & Humphrey, S. M. (2014). Microwave Synthesis of Classically Immiscible Rhodium-Silver and Rhodium-Gold Alloy Nanoparticles: Highly Active Hydrogenation Catalysts. *ACS Nano*, *8*(11), 11512–11521.

Garron, A., Lázár, K., & Epron, F. (2006). Characterization by Mössbauer spectroscopy of trimetallic Pd-Sn-Au/Al2O3 and Pd-Sn-Au/SiO2 catalysts for denitration of drinking water. *Applied Catalysis B: Environmental*, *65*(3-4), 240–248.

Garron, A., Lázár, K., & Epron, F. (2005). Effect of the support on tin distribution in Pd-Sn/Al2O 3 and Pd-Sn/SiO2 catalysts for application in water denitration. *Applied Catalysis B: Environmental, 59*(1-2), 57–69.

Gumuslu, G., Kondratyuk, P., Boes, J. R., Morreale, B., Miller, J. B., Kitchin, J. R., & Gellman, A. J. (2015). Correlation of Electronic Structure with Catalytic Activity: H2 − D2 Exchange across Cu x Pd 1 − x Composition Space, *ACS Catalysis,* 5, 3137-3147.

Guy, K., Xu, H., Yang, J. C., Werth, C. J., & Shapley, J. R. (2009). Catalytic Nitrate and Nitrite Reduction with Pd-Cu/PVP Colloids in Water: Composition, Structure, and Reactivity Correlations. *Journal of Physical Chemistry C*, *113*(19), 8177–8185.

Heck, K. N., Nutt, M. O., Alvarez, P., & Wong, M. S. (2009). Deactivation resistance of Pd/Au nanoparticle catalysts for water-phase hydrodechlorination. *Journal of Catalysis*, *267*(2), 97–104.

Kapoor, A., and T. Viraraghavan (1997). Nitrate removal from drinking water-review. *Journal of Environmental Engineering***,** 123, 371-380.

Kunal, P., Li, H., Dewing, B., Zhang, L., Jarvis, K., Henkelman, G., Humphrey, S. (2016). Microwave-Assisted Synthesis of $Pd_xAu_{(100–x)}$ Alloy Nanoparticles: A Combined Experimental and Theoretical Assessment of Synthetic and Compositional Effects upon Catalytic Reactivity. Manuscript in review.

Lehman, S. G., Badruzzaman, M., Adham, S., Roberts, D. J., & Clifford, D. A. (2008). Perchlorate and nitrate treatment by ion exchange integrated with biological brine treatment. *Water Research, 42*(4-5), 969–976.

Liu, J., Choe, J. K., Wang, Y., Shapley, J., Werth, C. J., Strathmann, T. (2015) A bio-inspired complex-nanoparticle hybrid catalyst system for aqueous perchlorate reduction: Rhenium speciation and its influence on catalyst activity, *ACS Catalysis*, 5, 511-522.

Liu, P., Norskøv, J. K., (2001). Ligand and Ensemble Effects in Adsorption on Alloy Surfaces, *Physical Chemistry Chemical Physics*, 3, 3814–3818.

Marchesini, F. A., Irusta, S., Querini, C., & Miró, E. (2008). Nitrate hydrogenation over Pt,In/Al2O3 and Pt,In/SiO2. Effect of aqueous media and catalyst surface properties upon the catalytic activity. *Catalysis Communications*, *9*(6), 1021–1026.

National Research Council, Committee on Toxicology. (1995). Nitrate and nitrite in drinking water. Washington DC: National Academies Press.

Nolan, B. T., & Hitt, K. J. (2006). Vulnerability of Shallow Groundwater and Drinking-Water Wells to Nitrate in the United States, 7834–7840.

Pintar, A., Batista, J., Levec, J., & Kajiuchi, T. (1996). Kinetics of the catalytic liquid-phase hydrogenation of aqueous nitrate solutions. *Applied Catalysis B: Environmental*, *11*(1), 81–98.

Pretzer, L. A., Song, H. J., Fang, Y. L., Zhao, Z., Guo, N., Wu, T., … Wong, M. S. (2013). Hydrodechlorination catalysis of Pd-on-Au nanoparticles varies with particle size. *Journal of Catalysis*, *298*, 206–217.

Qian, H., Zhao, Z., Velazquez, J. C., Pretzer, L. A., Heck, K. N., & Wong, M. S. (2014). Supporting palladium metal on gold nanoparticles improves its catalysis for nitrite reduction. *Nanoscale*, *4*, 358–364.

Sanchez-Echaniz, J., Benito-Fernandez, J., & Mintegui-Raso, S. (2001). Methemoglobinemia and Consumption of Vegetables in Infants. *Pediatrics*, *107*(5).

Sárkány, A., Horváth, A., & Beck, A. (2002). Hydrogenation of acetylene over low loaded Pd and Pd-Au/SiO2 catalysts. *Applied Catalysis A: General*, *229*(1-2), 117–125.

Shuai, D., McCalman, D. C., Choe, J. K., Shapley, J. R., Schneider, W. F., & Werth, C. J. (2013). Structure Sensitivity Study of Waterborne Contaminant Hydrogenation Using Shape- and Size-Controlled Pd Nanoparticles. *ACS Catalysis*, *3*(3), 453–463.

Shuai, D., Choe, J. K., Shapley, J. R., & Werth, C. J. (2012). Enhanced activity and selectivity of carbon nanofiber supported Pd catalysts for nitrite reduction. *Environmental Science & Technology*, *46*(5), 2847–55.

Shuai, D., Chaplin, B. P., Shapley, J. R., Menendez, N. P., Mccalman, D. C., Schneider, W. F., & Werth, C. J. (2010). Enhancement of oxyanion and diatrizoate reduction kinetics using selected azo dyes on Pd-based catalysts. *Environmental Science and Technology*, *44*(5), 1773–1779.

Sinfelt, J. H. (1977). Catalysis by Alloys and Bimetallic Clusters. *Accounts of Chemical Research*, *10*(17), 15–20.

Soares, O. S. G. P., Órfão, J. J. M., & Pereira, M. F. R. (2008). Activated Carbon Supported Metal Catalysts for Nitrate and Nitrite Reduction in Water. *Catalysis Letters*, *126*(3-4), 253–260.

Squillace, P. J., Scott, J. C., Moran, M. J., Nolan, B. T., & Kolpin, D. W. (2002). VOCs, Pesticides, Nitrate, and Their Mixtures in Groundwater Used for Drinking Water in the United States. *Environmental Science & Technology*, *36*(9), 1923–1930.

Stamenkovic, V., Mun, B. S., Mayrhofer, K. J. J., Ross, P. N., Markovic, N. M., Rossmeisl, J., & Nørskov, J. K. (2006). Changing the Activity of Electrocatalysts for Oxygen Reduction by Tuning the Surface Electronic Structure, 2897–2901.

USEPA (2007). Nitrates and nitrites toxicity and exposure assessment for children's health chemical summary, EPA TEACH databases, Washington, DC.

Venezia, A. M., La Parola, V., Deganello, G., Pawelec, B., & Fierro, J. L. G. (2003). Synergetic effect of gold in Au/Pd catalysts during hydrodesulfurization reactions of model compounds. *Journal of Catalysis*, *215*(2), 317–325.

Wang, L., Chen, A., Wang, A., Condit, W. (2011). Arsenic and Nitrate Removal from Drinking Water by Ion Exchange: USEPA Demonstration Project at Vale, OR. Final Performance Evaluation Report, USEPA, Cincinnati, OH

Weyer, P. J., Cerhan, J. R., Kross, B. C., Hallberg, G. R., Kantamneni, J., Breuer, G., … Lynch, C. F. (2001). Municipal Drinking Water Nitrate Level and Cancer Risk in Older Women: The Iowa Women's Health Study. *Epidemiology*, *11*(3), 327–338.

Witońska, I., Karski, S., & Gołuchowska, J. (2007). Kinetic studies on the hydrogenation of nitrate in water using Rh/Al2O3 and Rh-Cu/Al2O3 catalysts. *Kinetics and Catalysis*, *48*(6), 823–828.

World Health Organization (2011a). Guidelines for drinking-water quality, fourth edition. Nitrates and Nitrites, pages 398-403. Geneva CH.

World Health Organization (2011b). Nitrate and Nitrite in Drinking-water: Background document for development of WHO Guidelines for Drinking-water Quality, pages 10-13. Geneva CH.

Yi, C. W., Luo, K., Wei, T., & Goodman, D. W. (2005). The composition and structure of Pd - Au surfaces. *Journal of Physical Chemistry B*, *109*(39), 18535–18540.

Zhao, Z., Fang, Y.-L., Alvarez, P. J. J., & Wong, M. S. (2013). Degrading perchloroethene at ambient conditions using Pd and Pd-on-Au reduction catalysts. *Applied Catalysis B: Environmental*, *140-141*, 468–477.

Zhang, L., Wang, A., Miller, J. T., Liu, X., Yang, X., Wang, W., … Zhang, T. (2014). Efficient and durable Au alloyed Pd single-atom catalyst for the Ullmann reaction of aryl chlorides in water. *ACS Catalysis*, *4*(5), 1546–1553.

Ziv-El, M. C., & Rittmann, B. E. (2009). Systematic evaluation of nitrate and perchlorate bioreduction kinetics in groundwater using a hydrogen-based membrane biofilm reactor. *Water Research*, *43*(1), 173–181.

Vita

Sarah Seraj was born in Dhaka, Bangladesh. After completing high school in Dhaka city, she joined the University of Texas at Austin, where she obtained her Bachelor of Science in Civil Engineering in 2014.

Permanent email: sarah.seraj@gmail.com

This thesis was typed by Sarah Seraj.